

Quantitative archaeoseismological investigation of the Great Theatre of Larissa, Greece

R. Caputo · K.-G. Hinzen · D. Liberatore ·
S. Schreiber · B. Helly · A. Tziafalias

Received: 29 June 2009 / Accepted: 16 August 2010 / Published online: 9 September 2010
© Springer Science+Business Media B.V. 2010

Abstract Larissa, the capital of Thessaly, is located in the eastern part of Central Greece, at the southern border of a Late Quarternary graben, the Tyrnavos Basin. Palaeoseismological, morphotectonic, and geophysical investigations as well as historical and instrumental records show evidences for seismic activity in this area. Previous investigations documented the occurrence of several moderate to strong earthquakes during Holocene time on active faults with recurrence intervals of a few thousand years. The historical and instrumental records suggest a period of seismic quiescence during the last 400–500 years. The present archaeoseismological research, based on a multidisciplinary approach is devoted to improve the knowledge on past earthquakes, which occurred in the area. This study focuses on damages observed on the walls of the *scene* building of the Great Theatre of Larissa. The Theatre was built at the beginning of the third century BC and consists of a semicircular auditorium, an almost circular arena and a main *scene* building. Archaeological and historical investigations document a partial destruction of the theatre during the second to first century BC. Recent excavations show that the building complex after it was repaired suffered additional structural damages, probably from seismic loading. The damages investigated in detail are displacements, rotations and ruptures of numerous blocks at the walls of the *scene* building. In order to test the earthquake hypothesis as cause of the damages a simplified

R. Caputo (✉)
Department of Earth Sciences, University of Ferrara, Ferrara, Italy
e-mail: rcaputo@unife.it

K.-G. Hinzen · S. Schreiber
Institute for Geology and Mineralogy, University of Cologne, Cologne, Germany

D. Liberatore
Department of Structural Engineering and Geotechnics, University of Rome “La Sapienza”, Rome, Italy

B. Helly
Maison de l’Orient Méditerranéen “Jean-Pouilloux”, Université Lyon-2, Lyon, France

A. Tziafalias
Department of Prehistorical and Classical Antiquities, Larissa, Greece

seismotectonic model of the Tyrnavos Basin and its surroundings was used with a composite earthquake source model to calculate synthetic seismograms at the Larissa site for various earthquake scenarios. Horizontal to vertical seismic ratio (HVSR) measurements in the theatre and its vicinity were used to estimate local site effects. The synthetic seismograms are then used as input accelerations for a finite element model of the walls, which simulates seismically induced in-plane sliding within the walls. Results show that some of the surrounding faults have the potential to produce seismic ground motion that can induce in-plane sliding of blocks. Model calculations were used to constrain the characteristics of the ground acceleration and infer the causative fault and earthquake by comparing the calculated and observed distribution of the displacements of the blocks. Ground motions with a PGA at the site of 0.62–0.82 g, which could be induced by an M 5.8–6.0 earthquake on the nearby Larissa Fault, would be sufficient to explain the damage.

Keywords Archaeoseismology · Thessaly · Ancient theatre · Cultural heritage · Seismic hazard

1 Introduction

Archaeoseismology is a young, ambitious discipline, which integrates contributions from a wide range of scientific fields. Early studies on archaeoseismology of the Mediterranean Region were first published during the turn of the nineteenth to the twentieth century (e.g. [De Rossi 1874](#); [Evans 1928](#)). Later on scientists began to use some archaeological information to improve the knowledge about ancient earthquakes and to study seismogenic reasons as a possible cause for the destruction and abandonment of settlements ([Nikonov 1988, 1996](#); [Stiros and Jones 1996](#); [Korjenkov and Mazor 1999](#); [Galadini et al. 2006a,b](#); [Caputo and Helly 2008](#)). For a long time different perspectives hampered the development of an archaeoseismological methodology (e.g. [Ambraseys 1971](#)). However from multidisciplinary projects and works a foundation for Archaeoseismology was developed ([Stiros and Jones 1996](#)). Since then also quantitative measures for the proposed seismic load at an archaeological site or the dimension of the causative earthquake(s) have been the focus of several studies (*i.e.* [Stiros and Jones 1996](#); [Hinzen and Schütte 2003](#); [Hinzen 2005](#); [Fäh et al. 2006](#); [Decker et al. 2006](#)).

This study presents archaeoseismological results from the Great Theatre of Larissa in Thessaly, Greece (Fig. 1), which has been systematically excavated in the past 15 years, using a multidisciplinary quantitative approach. This monument shows clear evidences of ground-motion-induced damages, which have been attributed to a Medieval-time historical earthquake ([Caputo and Helly 2005a](#)).

The Great Theatre is located in the Pinios River alluvial plain (Fig. 1b) flooring the Middle-Late Quaternary Tyrnavos Basin ([Caputo and Pavlides 1993](#)). The graben is bordered by few major active faults (Fig. 2) previously investigated by [Caputo \(1995\)](#) and [Caputo et al. \(2006\)](#), and references therein). Based on a qualitative approach, [Caputo and Helly \(2005a\)](#) conclude that one of the faults bordering the Tyrnavos Basin was possibly responsible of the observed damages at the Great Theatre. The present research represents an attempt to quantitatively answer the following key questions. First, are earthquakes in the Tyrnavos Basin strong enough to explain the observed damages in the Great Theatre of Larissa? Second, do block displacements observed in the walls of the *scene* building allow narrowing down the ground motion parameters? Third, are the existing input data sufficient to use deterministic engineering seismological models to explain the damages in the theatre building?

2 The Great Theatre of Larissa

The monument is the largest example of a theatre built entirely from stone in Central Greece (Fig. 1). It was built following the traditional plan and architecture of the Classical time but during the beginning of the third century BC (Early Hellenistic). The monument consists of a semicircular area of stepping seats (*koilon*) ending at, and laterally supported by, two thick

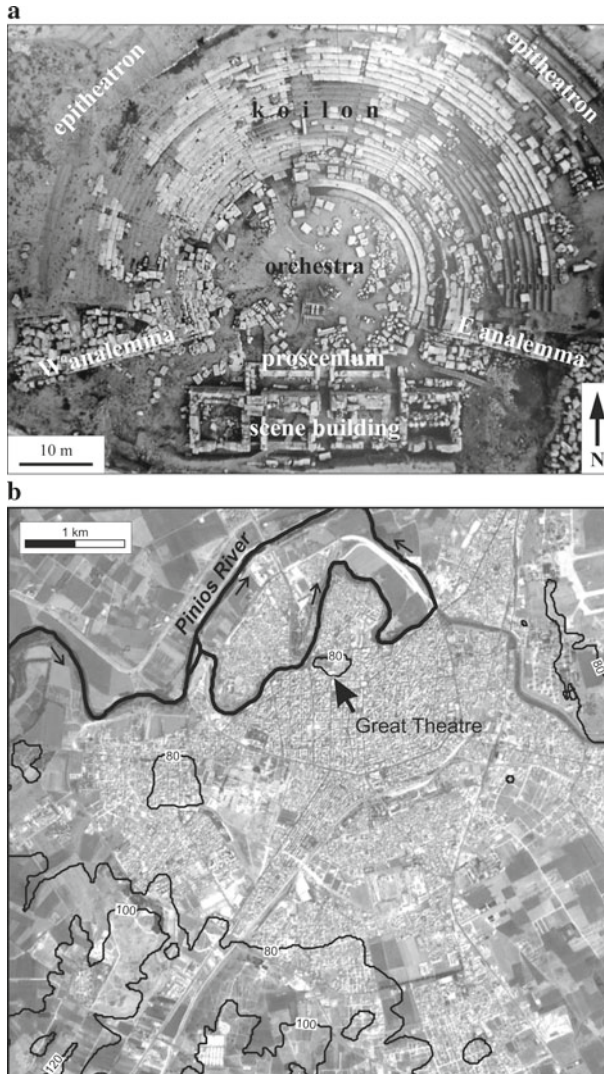


Fig. 1 **a** Aerial photo of the Great Theatre of Larissa during the initial stages of the ongoing excavations. The major architectonic elements of the monument are indicated. (Photo, A. Efthimiopoulos). **b** Location of the theatre within the modern town of Larissa expanding on the Late Quaternary alluvial plain and the northern slopes of the Central Hills (Caputo 1990). Pinios River (thick line) and contour lines a.s.l. (thin lines) are drawn on a GoogleEarth photo. The ancient course of the river corresponds to the eastern branch meandering closer to the theatre

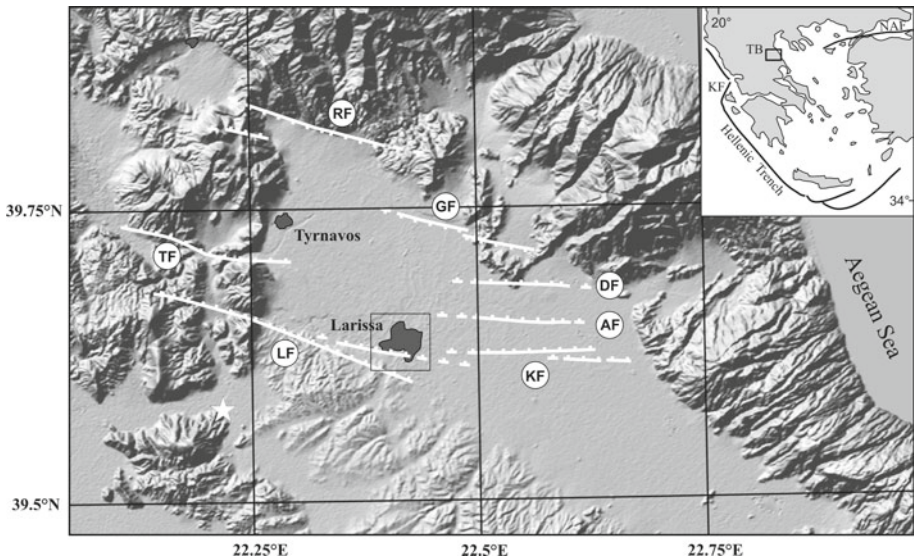


Fig. 2 Digital elevation model of the Tyrnavos Basin and surrounding areas in Thessaly, Greece. Major active faults in the basin are: *LF* Larissa Fault, *KF* Kastri Fault, *AF* Asmaki Fault, *DF* Dimitra Fault, *GF* Gyrtoni Fault, *RF* Rodia Fault, and *TF* Tyrnavos Fault. Location of the major towns of Larissa and Tyrnavos are shown. The *white star* indicates the location of the quarries for the Triassic crystalline limestone used for the Great Theatre of Larissa. The *box* enclosing Larissa indicates the location of Fig. 1b. The *inset map* shows the general tectonic setting of the broader Aegean Region and the location of the Tyrnavos Basin (TB). *NAF* North Anatolian Fault, *KF* Kefallinia Fault

walls (*analemma*). Fourteen series of seats have been preserved and only the higher part (*epitheatron*) is almost completely lost due to later spoliation. During its operation, the Great Theatre could receive as much as 10,000 spectators. At the centre, there is a circular open space (*orchestra*) and in the southern sector the main building (*scene*). The *scene* building consists of two central and two wing rooms. The walls of the *scene* building are made of seven courses of blocks (*assises*), with a total thickness of about 1.2 m. The northern walls of the two central rooms have been particularly strengthened and reach a thickness of 1.9 m. The *koilon* is located on the gentle slope of an artificial hill consisting of several meters-high stratified anthropogenic layers (Fig. 1b), while the *orchestra* and *scene* were built on the flat-lying alluvial deposits of the Pinios River with possible sedimentary contributions from the streams running off the northern Central Hills (Fig. 1b).

The *koilon* and the visible parts of the *scene* building were built from Triassic crystalline limestone cut from quarries 20–25 km west of Larissa (Fig. 2). The remaining stone blocks were extracted from the Pliocene Tyrnavos Formation (Caputo 1990) mainly consisting of oolitic calcarenites and referred to by archaeologists as ‘porolithos’ (i.e. porous rock). During the second century BC in the frontal section of the *scene* building a Doric style *proscenium* was added. At the beginning of the Imperial time (last 10 years of the first century BC), the theatre underwent a deep re-handling due to a partial destruction attributed to a seismic event (Caputo and Helly 2005a). This event occurred between the second half of the second century, and the middle of the first century BC.

The operation of the Great Theatre lasted until the end of the third century AD. The fact that after this time the building was not dismantled for its marbles and squared stones or for the lead within the junctions between blocks, which commonly occurred in ancient and

modern times, suggests that the monument was partially covered starting soon after its abandonment. Radiocarbon analyses of samples collected from a stratigraphic section excavated few metres south of the *scene* building consisting of alternating alluvial and anthropogenic deposits provide ages between 430 and 1220 AD, thus supporting the suggested evolution (Caputo and Helly 2005a).

3 Building and damage

Excavation of the theatre revealed several direct evidences of damages that can be subdivided into five groups (Fig. 3). Figure 3a shows the widespread horizontal in-plane sliding effects of blocks of the *scene* building. While unaffected blocks are in perfect contact with their neighbours, displaced blocks show opened gaps between 1 and >30 mm. Several monolithic columns from crystalline limestone (Fig. 3b) of the *proscenion*, 2.8 m high, show identical oblique shear fractures dipping to the North. These ruptures have all in common that they occurred at a height of ca. 0.5–1 m. Besides in-plane sliding, block rotations and off-plane sliding also contribute to the damage pattern (Fig. 3c). Blocks from the *scene* building and the *analemma* show rotations up to 2.5° , corresponding to 8 cm of absolute movement, as well as fracturing. The example in Fig. 3d is the sill of the western central room. This massive

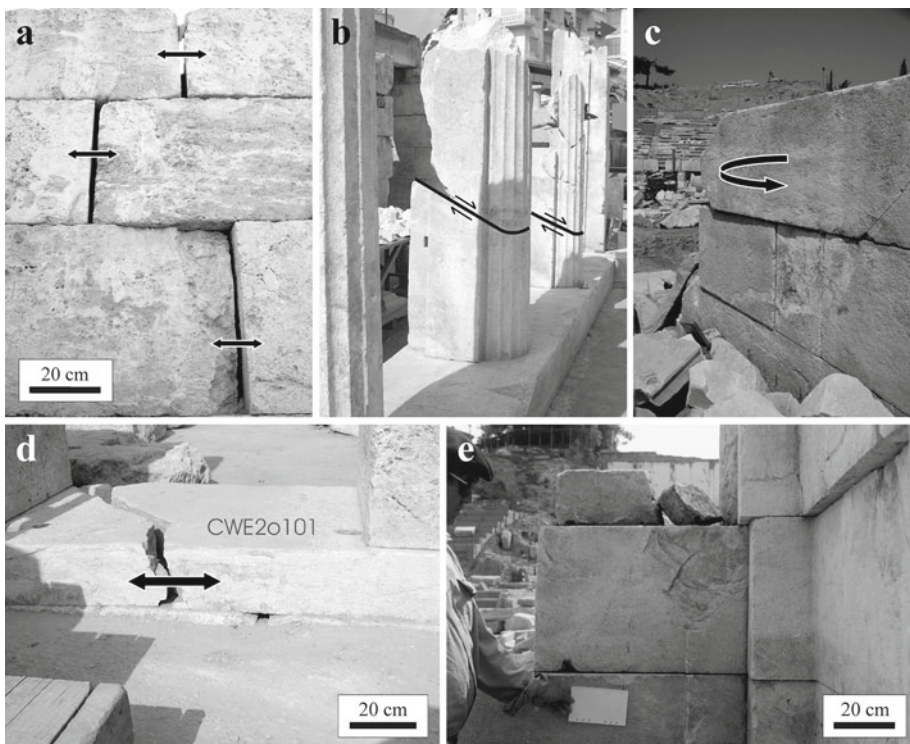


Fig. 3 Typical structural damages in the Great Theatre of Larissa: **a** in-plane block sliding at the *scene* building, **b** shear fractures in columns of the *proscenion*, **c** rotation of blocks, **d** tensional fracturing of blocks and sills, here at the door to the central western room, and **e** spalling of block corners. The *arrows* indicate the direction of movement. (Photos, R. Caputo)

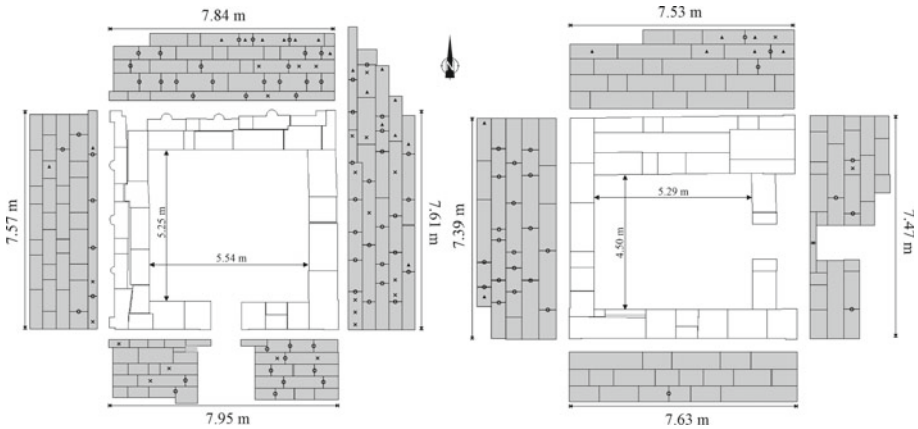


Fig. 4 Floor plan and wall structure, as seen from outside, of the western wing room (*left*) and the western central room (*right*) of the *scene* building of the Great Theatre of Larissa. The still existing blocks of the individual walls are indicated. *Circles*: opening (*in-plane sliding*) between blocks; *crosses*: tensional fractures across block; *triangles*: rotated block (*off-plane sliding*). See also Table 1. Not all damages shown in Table 1 are visible in Fig. 4

Table 1 Damage categories

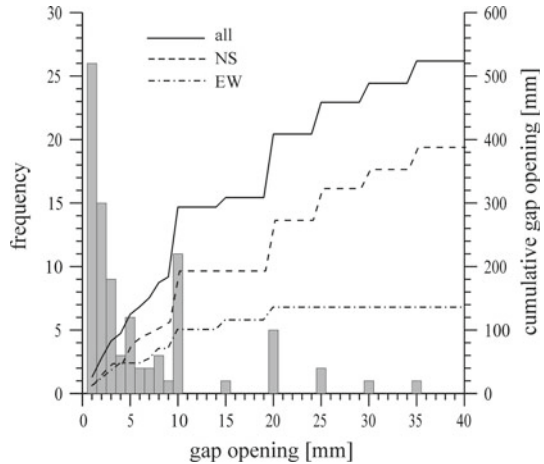
<i>Scene</i> building wall	In-plane sliding (%)	No. of joints	Block rotation and off-plane sliding (%)	No. of blocks	Block fracturing (%)	No. of blocks
Western wing room, N wall	47.5	28	12.5	8	12.5	8
Western wing room, E wall	76.1	35	17.3	9	32.7	17
Western wing room, S wall	42.7	13	0.0	0	23.5	10
Western wing room, W wall	23.2	13	3.0	2	8.3	5
Western central room, N wall	6.3	3	15.8	9	1.8	1
Western central room, E wall	18.8	4	6.4	3	16.5	6
Western central room, S wall	4.0	1	0.0	0	0.0	0
Western central room, W wall	79.2	19	10.0	3	3.0	1

The three major damage categories recognized in the *scene* building of the Great Theatre of Larissa (Figs. 3, 4). Values indicate the percentage of the affected blocks for each wall

block shows a tensile fracture with a gap opening of ca. 55 mm indicating strong horizontal forces exceeding the tensile strength of the material. Another strong indicator for seismogenic origin of the damages is spalling at the edges of blocks (Fig. 3e), most likely due to dynamic interaction with the neighbouring blocks. In summary, all the above described damages are likely associated with a seismically induced ground motion because none of the observed and described features can be simply attributed to creep movements, static settling nor to human activities.

The present research focuses on the two western rooms of the *scene* building because they are the most well preserved. Figure 4 shows the structure of the walls and floor plans of the western wing room and the western central room of the *scene* building. After all damages had been documented in the field, a database with the location and damage situation for each individual block was set up. Table 1 summarizes the extent of the damage to the walls of

Fig. 5 Histogram (gray bars) and cumulative curve (black line) of the measured *in-plane sliding* of blocks in the outer walls of the two western rooms (Fig. 4) of the *scene* building of the Great Theatre of Larissa. Dashed and dashed-dotted lines represent the cumulative distribution of the NS- and EW-trending walls, respectively



these two rooms for three damage categories: in-plane sliding, block rotation and off-plane sliding, and block fracturing. The values reported in Table 1 represent the percentages of the affected blocks, while their location relative to the external blocks of the walls are represented in Fig. 4. The walls of the western wing room suffered more damage than those of the western central room, for two main reasons: the western central room is more ‘internal’ within the building, while the northeastern corner of the western wing room was connected to the *analemma* of the theatre and this might have caused a differential behaviour and hence additional damage during earthquakes.

Figure 5 shows the frequency of occurrence of gap openings, which range from 1 to 35 mm, for all outside walls of the two rooms. The sum of all openings is 524 mm for the eight walls. The peak in the distribution at a gap opening of 10 mm must be regarded as an artifact; here openings close to 1 cm were documented as 10 mm. However in the sum over all readings this artifact should even out.

While all walls suffered some damage, a clear directional pattern cannot be recognized. Indeed, Fig. 5 also shows the cumulative gap opening separately for the NS- and EW-trending walls. The difference in the two perpendicular directions is most probably caused by differences in the wall structure, though ground motion directivity could also have played a role.

At this regard, we focus on the cumulative gap opening because it is a much more general parameter than individual block movements. The use of a more robust parameter like this is recommended due to the uncertainties in the input parameters and the simplifications applied to the models. Similarly, due to the overall damage distribution we modelled the general behaviour of the in-plane sliding in the two rooms, rather than regarding each wall individually.

4 Historical and instrumental seismicity

Historical and instrumental seismicity of the Thessaly and the Tyrnavos Basin has been recently revised and described in detail (Caputo and Helly 2005a; Caputo et al. 2006). Inscriptions dated at the end of the third century BC give the oldest known written hints to Thessaly

earthquakes. Among the historical earthquakes with written evidence three are listed with their epicenter in the Larissa area in 1731, 1781, and 1892 with maximum macroseismic intensities between VI and VII (Papaioannou 1981; Papazachos and Papazachou 1997). The instrumental record starts in 1911 and lists 9 earthquakes with magnitudes 6.0 or above. The strongest among these is the 1954 Sophades earthquake with a surface wave magnitude M_s of 6.7. In 1941 an earthquake with the epicenter in the Larissa area and M_s 6.1 is the only instrumental event that certainly occurred in the Tyrnavos Basin. The cumulative distribution of both instrumental and historic seismicity suggests a good catalogue completeness for $M > 6.0$ within Thessaly, since the seventeenth century (Caputo and Helly 2005a). Taking also into account that during the fifteenth century AD the city of Larissa, which was almost abandoned at that time, was occupied by the Ottomans and renamed Yenisher (meaning “new town” in Turkish) and no specific record exists concerning strong earthquakes, it is likely that the Tyrnavos Basin and particularly Larissa were not affected by important ground shaking events in the past 4–5 centuries, with the only exception of the 1941 event.

5 Modelling procedure

Deducing the characteristics of ground motions from the associated structural damages is a complex and challenging task. Due to the complex nature of the three-dimensional ground motion, soil-building interaction and the strong non-linear behaviour of the structure, it is unpromising to interpret structural deformation in detail (Hinzen 2008). However a general understanding of vibration levels, duration and frequency characteristics may be achieved if the response of structural elements is studied more macroscopically. In this study we try to estimate a lower bound of the seismic ground motion that is necessary to induce horizontal block sliding in the walls of the Great Theatre. As an overall measure for the deformation level, we regard the cumulative gap opening in the two western *scene* buildings considering only the outer walls, as only these are completely accessible. Accordingly, all gap openings measured for the outer walls are summed up. The shape and total cumulative gap opening (Fig. 5) is a much more general expression of the damage than individual gap openings that could be influenced by local effects.

Different strategies can be followed in order to model site-specific seismic ground motions. One way of estimating the dynamic load of the theatre could be scaling records from smaller earthquakes (*i.e.* Andrews 1986; Boatwright et al. 1991) or using empirical attenuation relations based on previously recorded earthquakes (Atkinson and Boore 2003; Scherbaum et al. 2006; Bommer et al. 2007).

However both procedures suffer from large uncertainties in the site specific loading from unknown geometry of the rupture with respect to the site, the recorded earthquake magnitude, seismic moment and stress drop of the recorded event versus the damaging earthquake and geologic conditions of the recording site(s) compared to the design site (Keaton 1999). As a comprehensive probabilistic treatment of the problem was beyond the scope of this study, we decided to follow a deterministic approach in which there is control over the model parameters even though they might be uncertain or an expert's guess.

In order to narrow down location and size of earthquake sources which might have been causative for the observed and documented damages, we followed a three-step deterministic approach: (1) develop a seismotectonic model of the main active faults affecting the Tyrnavos Basin, (2) calculate site specific strong motion seismograms for the site of the Great Theatre, (3) estimate the permanent displacements of blocks of the *scene* building under seismic loading and compare these displacements to the observations.

Table 2 Fault parameters

Fault		Latitude	Longitude	Length (km)	Width (km)	Dip	Strike
Rodia	RF	39.83°N	22.25°E	15	10	50°S	109°
Ghyrtoni	GF	39.74°N	22.44°E	12	8	60°S	101°
Tyrnavos	TF	39.73°N	22.16°N	13	9	50°N	282°
Larissa	LF	39.66°N	22.23°E	18	12	60°N	285°
Asmaki	AF	39.66°N	22.49°E	10	7	60°N	272°
Dimitra	DF	39.69°N	22.49°E	10	7	60°N	276°
Kastri	KF	39.63°N	22.53°E	12	8	60°N	269°

Surface location and principal geometrical parameters of the active faults in the simplified seismotectonic model of the Tyrnavos Basin (Fig. 2). Latitude and longitude are referred to the western corner of the fault trace. Dip and strike are in the convention of [Aki and Richards \(1980\)](#) source orientation for all earthquakes

6 Potential earthquake sources

The seismotectonic model of Thessaly (Fig. 2) was developed on the basis of geological, morphotectonic, palaeoseismological and geophysical researches ([Caputo 1995](#); [Caputo and Helly 2000, 2005b](#); [Caputo et al. 1994, 2003, 2004, 2006](#)). It is shown on a digital elevation model (DEM) from data of the NASA Shuttle Radar Topography Mission (SRTM; <http://www2.jpl.nasa.gov/srtm/>). The principal seismotectonic parameters of the seven major active faults are listed in Table 2. Fault dimensions are given on the basis of instrumental data from the US Geological Survey, the Geodynamic Institute of the National Observatory of Athens and [Kementzetzidou \(1996\)](#), the estimated depth of the seismogenic zone is 5–15 km. All faults are assumed to be emergent structures, and hence associated with linear morphogenic earthquakes ([Caputo 2005](#)).

Based on these active faults several earthquake scenarios were developed. The maximum magnitudes and seismic moments of each source were derived from the empirical relations between the surface rupture length and magnitude proposed by [Pavlidis and Caputo \(2004\)](#) and [Wells and Coppersmith \(1994\)](#) assuming that the entire fault was reactivated. Table 3 lists the parameters of 10 selected earthquake scenarios, which were used in the numerical modelling.

7 Composite source model

Synthetic strong motion seismograms of the scenario earthquakes in the Tyrnavos Basin were calculated with a composite seismic source model ([Zeng et al. 1994](#); [Keaton 1999](#)). The approach follows two steps: we first calculate the elastodynamic Green's function between the source and the site of interest and subsequently superimpose the wavelets from circular subsources distributed on the rupture plane. Green's functions are based in on a one-dimensional model of the crust (Fig. 6). Depth distribution of velocities, densities, and quality factors for the 1D model were taken from CRUST 5.1 and 2.0 ([Mooney et al. 1998](#); [Bassin et al. 2000](#)) for the general structure of the crust in North-West Greece and regional data for Thessaly from [Seber et al. \(2001\)](#), [Zelt et al. \(2005\)](#), [Drakatos et al. \(2005\)](#) as well as [Press \(1966\)](#) and [Knödel et al. \(1997\)](#).

Based on stratigraphic information from the archaeological excavations and HVSR measurements within the Theatre and its surroundings, a low velocity layer of a total

Table 3 Modelled faults

Fault	Modelled M_w	Rupture length (km)	Epical distance(km)	Hypocentral depth (km)	PGA (g)	Cumulative gap opening (mm)
Tyrnavos	6.5	13.0	20	10.6	0.73	128
Rodia	6.6	15.1	14	9.8	0.58	119
Gyrtoni	6.4	12.0	11	9.9	0.76	69
Dimitra	6.3	10.0	14	10.6	0.59	300
Larissa	6.7	18.0	10	11.9	1.32	5700
	6.0	5.6	7	10.7	0.83	1278
	5.9	4.7	7	10.1	0.72	372
	5.8	3.9	7	10.0	0.65	280
	5.7	3.3	2	10.0	0.28	188
	5.6	2.7	2	10.0	0.27	54

Fault parameters used for the composite source model and producing the ten selected earthquake scenarios. See also Figs. 7 and 8. Dimensions given at a +100 m are those used in the calculations, though uncertainty is obviously larger than that. Epicentral distance is measured assuming the hypocenter is located at the center of the reactivated fault plane

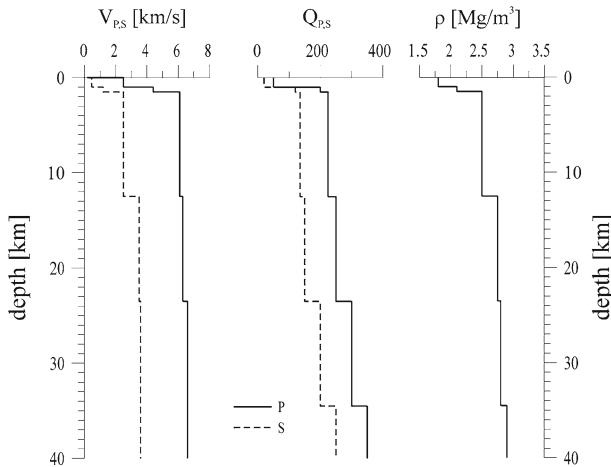


Fig. 6 Distribution of P- and S-wave velocities, quality factors, and density with depth for the Tyrnavos Basin based on the data referenced in the text (see text for details)

thickness of 5 m was introduced where the upper 2 m, representing artificial fill show a shear wave velocity of 170 m/s. Underneath partially compacted sediments with velocities above 1,000 m/s were assumed based on regional geological studies of the Tyrnavos Basin (Sogreah 1974; Caputo 1990; Caputo et al. 1994; Oliveto et al. 2004).

In order to simulate extended sources, circular subsources are distributed on a rectangular rupture plane. The size and location of the subsources is varied randomly between predefined limits. The activation time of the subsources during the rupture process is dependent on an assumed rupture velocity, in our case 80% of the shear wave velocity, and the location of the hypocenter on the rupture surface. Through variation of the latter, uni- or bidirectional rupture

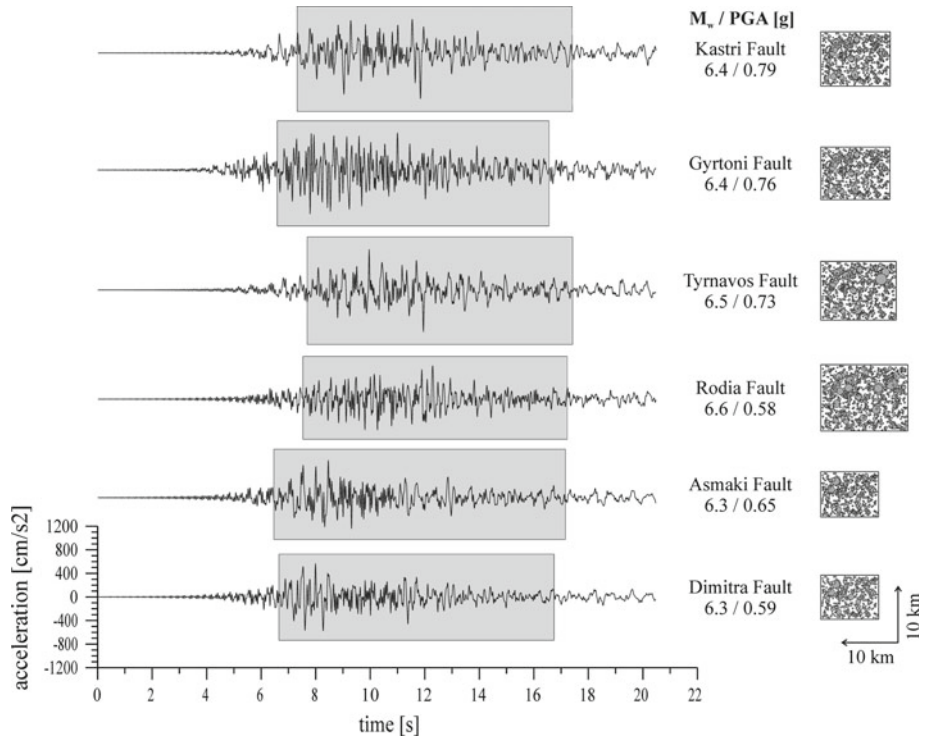


Fig. 7 Synthetic accelerograms of six earthquake scenarios on faults in the Tyrnavos Basin for the site of the Great Theatre of Larissa. Numbers at the *right side* of the seismograms give the moment magnitude and the PGA in g. The *gray-shaded* sections are the time windows between 5 and 95% of the Arias intensity. Fault names are indicated. In the *right column* the distribution of the subsources on the rupture plane is shown for each earthquake. For clarity of the plot only ca. 10% of the total number of subsources is plotted

spreading can be modeled. Size and number of the subsources are adjusted to finally meet the target seismic moment or moment magnitude. Dip values were assumed to be 50°–60° (Table 2), while based on faults’ strike and present-day stress field orientation (e.g. [Reinecker et al. 2005](#)), the rake is assumed –85° in the convention of [Aki and Richards \(1980\)](#) for all earthquakes. Stress drop of the subfaults was varied between 6 and 8 MPa. Figures 7 and 8 show the synthetic seismograms for the earthquake scenarios from this study and the sub-source distribution on the fault plane. The seismograms in Fig. 7 were calculated for the Kastri, Gyrtioni, Tyrnavos, Rodia, Asmaki, and Dimitra Faults, assuming the largest possible rupture plane in each case and producing peak ground accelerations at the Larissa site from 0.58 to 0.79 g. In Fig. 8, seismograms for earthquake scenarios on the Larissa Fault are shown for six different magnitudes ranging from 5.6 to 6.7, causing peak ground accelerations at the Great Theatre of Larissa between 0.27 and 1.32 g, respectively.

8 Finite elements model

The Finite Element (FE) model of the *scene* building walls is based on 2D linear elastic elements representing the blocks, and contact elements between the blocks. The latter are: a) interface elements, connecting the block elements vertically to their neighbours and the earth

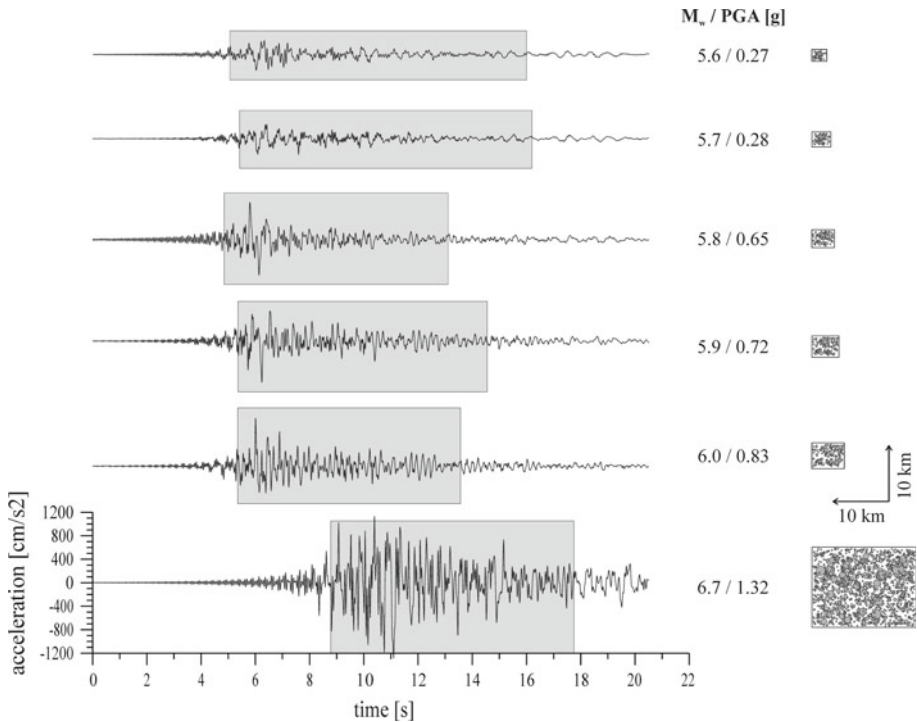


Fig. 8 Synthetic accelerograms of six earthquake scenarios on the Larissa Fault for the site of the Great Theatre. Numbers at the *right side* of the seismograms give the moment magnitude and the PGA in g. The *gray-shaded* sections are the time windows between 5 and 95% of the Arias intensity. In the *right column* the distribution of the subsources on the rupture plane is shown for each earthquake. For clarity of the plot only ca. 10% of the total number of subsources is plotted

surface, respectively, which account for monolateral contact and friction along horizontal surfaces (Psycharis and Jennings 1983; Grimaldi et al. 1991), and b) gap-elements which account for the monolateral contact between blocks of the same course along their vertical surfaces (D’Asdia and D’Ayala 1991).

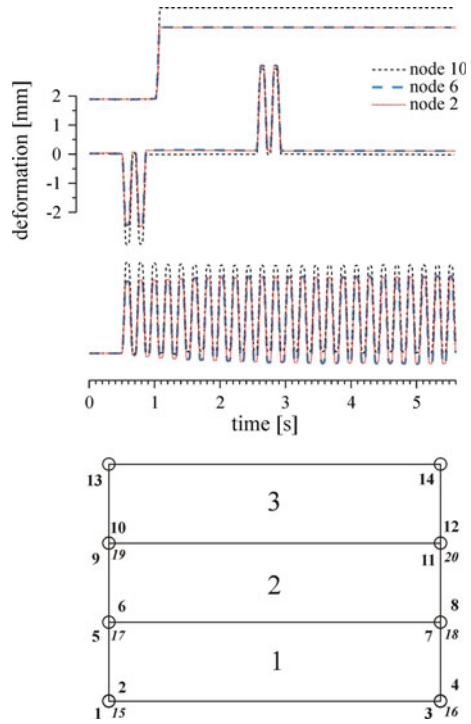
The FE model employed can be regarded as an adaptation to the problem under study of the more general Discrete Element Model (DEM), which in addition accounts for general changes of system configuration, as well as births and losses of contacts between blocks (Cundall and Strack 1979). Examples of application of the DEM to ancient block structures can be found in (Giuffrè et al. 1995; Pagnoni 1995; Chetouane et al. 2008). The FE calculations were made with the program ADA developed by Liberatore et al. (1998).

The modulus of elasticity of the block material was set to 186.7 GPa, with a density of $1.7 \cdot 10^3 \text{ kg/m}^3$ and a Poisson ratio of 0.16.

The horizontally oriented interface elements are combinations of vertically and horizontally oriented springs. The vertical springs transmit the normal forces between the stacked blocks. Frictional forces of the in-plane sliding are modeled by the horizontal springs according to a reduced Coulomb law

$$s_h = f r_v$$

Fig. 9 A simple 3-block FE model (*bottom*) was used to study the movements due to simple excitation functions. Large numbers are block labels and small numbers are node labels, which are in *italics* for auxiliary nodes for the interface elements. The three diagrams in the top show the relative displacement of nodes 2, 6 and 10, on the *lower left* corner of the first, second, and third block, respectively due to excitation by a spike-function, reversed sinusoidal impulses and a monochromatic sinusoidal acceleration with a frequency of 5 Hz (*top to bottom*), all with 1 g maximum amplitude



where s_h is the strength of the horizontal spring; r_v is the force in the vertical spring and f is the friction coefficient, set to 0.6 according to the results of sliding tests on inclined plane carried out on small scale marble blocks collected from the same ancient quarry used for the construction of the Great Theatre of Larissa (Fig. 2). On the other hand, based on numerical modelling, Hinzen (2008) showed that for numeric models of two columns, one composed of 7 drums and one monolithic, a variation of the static coefficient of friction between 0.3 and 0.9 does not significantly influence the toppling behaviour.

Finally, the gap-elements account for the opening and closing of gaps between blocks of the same course, due to differential sliding. The FE model of the walls of the *scene* building was developed by Sarubbi (2005).

Before the dynamic loading is applied to the model, a static analysis is carried out under vertical loads and all static forces are calculated.

Prior to the calculation of the deformations in the *scene* building walls induced by the scenario earthquakes, test calculations were made to study the performance of the 2D-FE model with a simple structure of only three blocks resembling the size of a typical *scene* building block (137 × 32 cm). Figure 9 shows the test FE model of 3 blocks and the calculated deformations from simple excitation acceleration functions: (1) spike, (2) sinusoidal pulses, and (3) monochromatic sinusoidal movements. The impulse of 1 g amplitude results in permanent horizontal displacements of the stack of blocks of 2.5 mm with respect to the ground-surface, blocks 1 and 2 show no differential movement and block 3 is displaced in total 3.5 mm.

In case of the sinusoidal impulses of 1 g maximum amplitude, the maximum relative displacements are almost exactly those of the spike excitation, however only a small permanent

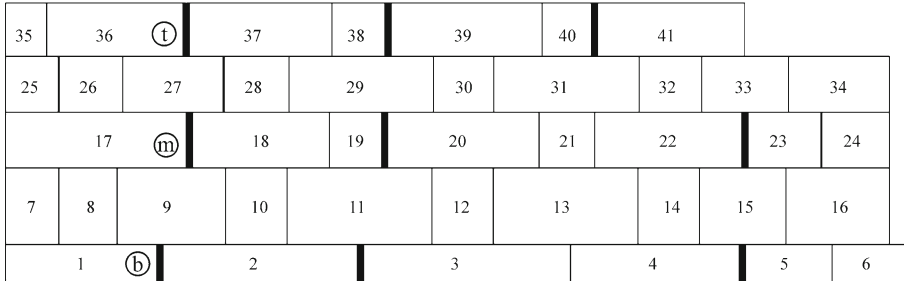
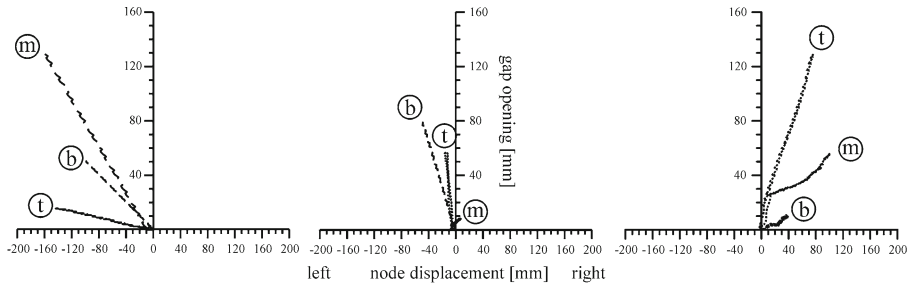


Fig. 10 The *bottom* shows the 2D FE model of the northern wall of the western wing room. The diagrams in the *top* of the figure show the opening of selected gaps versus the *horizontal* movement of the block at the *left side* of that gap. The corresponding gaps are indicated by the heavy lines in the block model, labeled *b*, *m*, and *t* for *bottom*, *middle* and *top* row of blocks, respectively

displacement of 0.1 mm is calculated for the lower two blocks in the opposite direction as the induced movement. Otherwise the blocks slide back into their original position. During the excitation with a monochromatic sinusoidal acceleration of 1g maximum amplitude, 5 Hz frequency and 5.44 s duration, the blocks 1 and 2 (Fig. 9) show a slight steady movement into the opposite direction of the initial ground motion, while inertial forces keep block 3 almost in a constant position.

The next test was performed with a model of a complete wall (northern wall of the western wing room) excited by the same ground motion. During this test the blocks at the left side of the wall shift to the left up to 160 mm (Fig. 10). The gap opening is largest in the middle with 125 mm; at the top the gap between blocks 36 and 37 opens only 12 mm. The movements on the right side are less than 100 mm and the gap width is similar to the left side, however here the largest gap is observed in the top course. In the center of the wall, movements and gap openings are significantly smaller than towards the edges. The blocks slide 50 mm maximum and gap openings are less than 80 mm. This result confirms typical seismic in-plane failure and damage patterns of masonry walls (Sarubbi 2005; Mistler et al. 2006).

9 Calculation results

The acceleration time series shown in Figs. 7 and 8 were used as excitation functions for the FE model. The actual length of the excitation function was 11.15 s in all cases, however assuring that the time window between 5 and 95% level of the Arias intensity was completely covered.

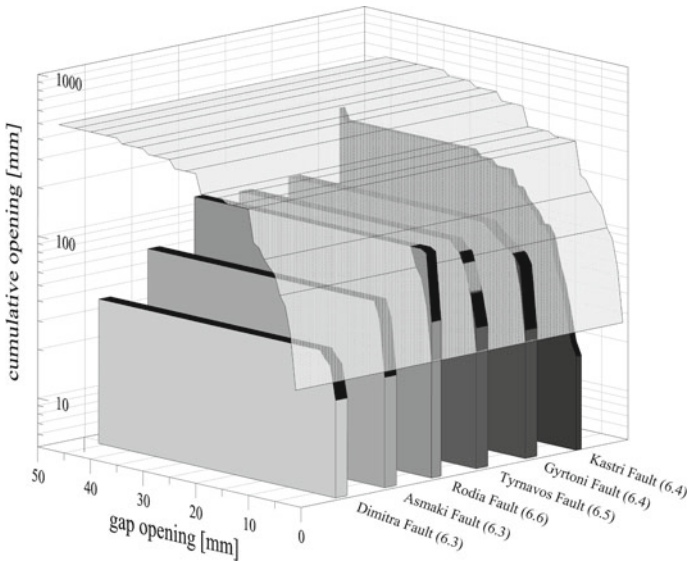


Fig. 11 Results of the model calculations of the displacements of blocks in the walls of the two western rooms of the *scene* building of the Great Theatre in Larissa. The cumulative displacements of all gaps on the walls for the six labeled earthquake scenarios are compared to observed values, which are shown as the *light gray* surface

Figure 11 summarizes the calculation results for the earthquake scenarios on the Kastri, Gyrtioni, Tyrmavos, Rodia, Asmaki, and Dimitra faults in form of cumulative displacement curves. These seismic sources have Joyner-Boore distance (*i.e.* Abrahamson and Shedlock 1997) between 6 and 12 km. Compared to the measured cumulative displacement curve, all calculation results show significantly smaller values of block sliding. For example, the largest earthquake on the Kastri Fault produces only 7% of the observed total displacement of 524 mm; the earthquakes on the Tynavos and Asmaki faults show ca. 24% of the total displacement, while the largest cumulative displacement is induced by the assumed maximum earthquake on the Dimitra Fault with 57% of the observed value. In contrast with the previous possible seismic sources, the sources assumed on the Larissa Fault all have 0 km Joyner-Boore distance. Figure 12 summarizes the results for the earthquake scenarios on the Larissa Fault. The total displacement induced by the earthquakes with magnitudes 5.6–5.9 increases from 10–70% of the observed value. Between magnitude 5.8 and 5.9 the number of gaps, which open a small amount increases significantly. For M 5.9 the cumulative displacement in the range of the smaller displacements (1–10 mm) is above the observed value (Fig. 12), however the additional wider gap openings, which further increase the cumulative value is not reached in the calculation. A further increase in the earthquake size to 6.0 leads to a calculated total displacement of the blocks of 2.4 times the observed value. Assuming the largest possible earthquake with a magnitude of 6.7 results in a 10-fold value of the calculated displacements, meaning that the ground motion from such an event would have destroyed the walls. It is evident, that any attempt to fine-tune parameters of the earthquakes, *i.e.* between M_w 5.8 and 6.0, to achieve a better fit between the calculated and observed cumulative displacements would be an overstressing of the model due to the overall uncertainties. As only the in-plane horizontal sliding of the blocks is covered by the FE-model and the strengthening effects of the corner stones are ignored, the comparison of observed and calculated displacement has to remain a

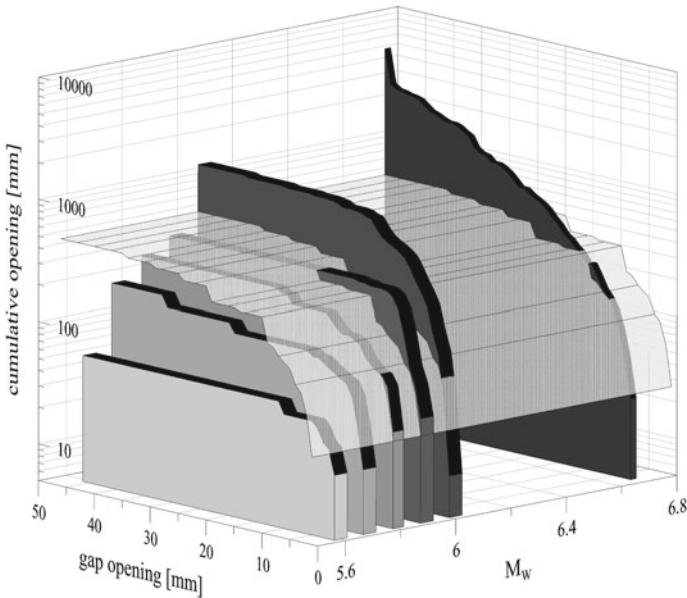


Fig. 12 Results of the model calculations of the displacements of blocks in the walls of the two western rooms of the *scene* building of the Great Theatre in Larissa. The cumulative displacements of all gaps on the walls for six earthquake scenarios on the Larissa Fault with M_w between 5.6 and 6.0 and for the largest assumed event with M_w 6.7 are compared to observed displacement values, which are shown as the *light gray* surface

coarse indicator of the building reaction. However, following the calculation results, none of the more distant faults bordering the Tyrnavos Basin (Fig. 2) has the potential to produce the observed block displacement with one event on the fault, even if the maximum rupture size of these faults is taken into account. On the other hand, an earthquake on the Larissa Fault, especially with a rupture extending in the eastern part of the fault and a Joyner-Boore distance of 0 km with a PGA of 0.65 g and a duration of the strong ground motion of 9 s (Table 3) is strong enough to displace the blocks in the *scene* building as much as observed in situ. There is a clear trend of increase of the total cumulative displacements with increasing peak ground acceleration for the earthquakes modeled on the Larissa Fault, at least above a threshold of 0.6 g, which probably depends on the assumed coefficient of friction. While a magnitude 5.6 earthquake on the Larissa Fault opens 11% of the modelled joints, a M 6.0 earthquake opens 80% and the worst case event of M 6.7 activates 94%.

10 Discussion

Seismogenic causes of the building damages observed and documented in the Great Theatre of Larissa were suggested and discussed qualitatively by Caputo and Helly (2005a), but no causative fault was proposed. The present research provides a step forward improving knowledge of the seismotectonics of the area. Indeed, based on a simple deterministic approach, the possible local earthquakes sources (Fig. 2; Table 2) and their dynamic loading at the site of the Great Theatre of Larissa (Figs. 7, 8; Table 3) are modelled. This allows constraining seismic scenarios to explain the observed damages. Geometry and size of the major active faults in the Tyrnavos Basin surrounding the town of Larissa are relatively well constrained

(e.g. [Caputo 1995](#)). However, in order to model site specific ground motion scenarios for the Theatre location, additional data about the subsurface structure and wave spreading conditions are necessary. Due to the lack of measurements like deep seismic profiles we had to make several assumptions about these data, introducing model uncertainties, which might be reduced in future studies.

As described previously ([Caputo and Helly 2005a](#)) and summarized above, several types of damages were observed in the Great Theatre of Larissa, which are typical for seismicogenic causes ([Mazor and Korjenkov 2001](#); [Korjenkov et al. 2006](#); [Galadini et al. 2006a](#)). However in this paper only the in-plane sliding of blocks from the *scene* building was modeled to get a start on numerical analysis of the building behaviour as the physics of the horizontal sliding is easier to describe than block rotation and the breaking of the columns (Fig. 3). The FE model of the *scene* building walls contains several simplifications and assumptions, which have to be taken into account when the calculation results are interpreted. For example, some of the blocks in the *scene* building wall are connected by vertical and/or horizontal iron anchors welded with lead to the stone block. It is not known, where exactly all of these are located within the walls and how many of these anchors are present in the building. These anchors have certainly influenced the sliding behaviour of wall blocks. Anchored blocks probably move as a unit at least up to a certain, so far unknown ground motion threshold, before the link is weakened or broken. Effects of these clamps are not considered by the model calculations in this paper. Although the comparison with similar ancient Greek monuments suggests that anchoring was applied only to some of the external blocks, the estimated damaging ground motion levels have to be regarded as a lower bound. Looking at the cumulative gap opening independent of the wall orientation is also a simplification, however acceptable as only the in-plane sliding of blocks was considered in the model.

All calculations for the faults more distant than the Larissa Fault were made for worst-case scenarios. Possible accumulation of block movements from several earthquakes were not studied in detail. However during the test calculations with a 3-block model (Fig. 9) and simple excitation functions for a wall of the *scene* building, we observed that it is not likely that a series of smaller earthquakes generates the same cumulative block sliding curves as a single strong earthquake. The complex ground motion from several earthquakes does not necessarily increase initially small gaps to larger gaps. This is also supported by the observation that a certain ground motion threshold has to be exceeded to generate gaps in the order of 30 mm or more. Indeed, for the earthquakes with rupture planes on the Larissa Fault only gaps smaller than 10 mm were calculated for magnitudes below 5.7. Ground motion from earthquakes with magnitudes less than 5.5 only produced gaps of 1–3 mm. The model calculations do not completely exclude the possibility that the current damage pattern is the result of several earthquakes, however in case of an activation of the Larissa Fault at least one of these earthquakes must have had a magnitude larger than 5.7.

In addition to the local faults bordering the Tyrnavos Basin, we also tested the possibility of block sliding at the *scene* building of the Great Larissa Theatre induced by a rather strong earthquake but on a more distant fault. Attenuation along the larger distances leads to smaller PGAs than the regional earthquakes, however, we wanted to test possible effects from the changed frequency content of the signals. The two tested examples are a magnitude 7.5 earthquake assumed on the Marmara Sea segment of the North Anatolian Fault and a magnitude 7.3 earthquake on the Kefallinia Fault along the western Ionian coast. In both cases ground motions were not large enough to produce the observed block movements due to the large distances of 400 and 150 km, respectively (Fig. 2).

The simplifications and uncertainties of some input parameters of the model do not allow deducing precise parameters of the causative earthquake, which damaged the Great Theatre of Larissa. However, a close earthquake, i.e. on the Larissa Fault with a minimum magnitude of 5.8–6.0, best explains the block-sliding distribution of the *scene* building walls.

11 Concluding remarks

The multidisciplinary quantitative approach presented in this paper and the results obtained from the numerical modelling, allow responding to the key questions posed in the Introduction. In particular, the first answer is certainly positive because most of the faults affecting the Tyrnavos Basin are capable of producing damages at the Great Theatre of Larissa, though not all of them are capable to generate the same distribution of cumulative gap openings in the walls.

Also for the second question posed, the answer is positive but only up to a limited degree of confidence due to the uncertainties intrinsic in the followed procedure and in the original information that was available. Based on the modelling results, an earthquake on the Larissa Fault is the most probable among the tested scenarios, while it is unlikely that any of the other faults bordering the Tyrnavos Basin caused the earthquake producing the observed damages at the Great Theatre of Larissa.

As concerns the third question, the input data were sufficient to study certain aspects of the reaction of selected parts of the building (in-plane sliding of blocks in two rooms). However this first simplifying approach neglects effects of clamping devices, off-plane movements as well as rotations and fractures. In order to study these more complex building behaviours more sophisticated models and in situ tests i.e. on the frictional parameters of the limestone blocks are necessary. Additionally the effect of uncertainties in the input data like the inelastic damping properties of the crust and the ground amplification as well as source parameters and model simplifications have to be further investigated. For future studies a probabilistic approach is desirable in which uncertainties of the model parameters are treated systematically.

The proposed high probability of re-activation of the Larissa Fault during the seventh to fifteenth century (Caputo and Helly 2005a) and the low probability that co-seismic movements on more distant faults caused the damage observed in the Great Theatre of Larissa should be considered in future local seismic hazard assessments. This also makes the Larissa Fault a target for future palaeoseismological investigations.

Acknowledgments Financial support came from the Deutscher Akademischer Austausch Dienst (DAAD, Vigoni D-04/47121) and the Conferenza dei Rettori delle Università Italiane (CRUI, Vigoni Project 2005). Parts of the study were financed by Deutsche Forschungsgemeinschaft (DFG) contract HI 660/2-1. Thanks to Marco Mucciarelli for discussions on the site effects.

References

- Abrahamson NA, Shedlock KM (1997) Overview. *Seismol Res Lett* 68:9–23
- Aki K, Richards PG (1980) *Quantitative seismology*. Freeman and Co, New York
- Ambraseys N (1971) Value of historical records of earthquakes. *Nature* 232:375–379
- Andrews DJ (1986) Objective determination of source parameters and similarity of earthquakes of difference size. In: Das S, Boatwright J, Scholz CH (eds) *Earthquake source mechanics*. American Geophysical Monograph, vol 37, pp 259–268
- Atkinson GM, Boore DM (2003) Empirical ground-motion relations for subduction-zone earthquakes and their application to cascadia and other regions. *Bull Seism Soc Am* 93:1703–1729
- Bassin C, Laske G, Masters G (2000) The current limits of resolution for surface wave tomography in North America. *EOS Trans AGU*, 81:F897

- Boatwright J, Seekins LC, Fumal TE, Liu H-P, Mueller CS (1991) Ground motion amplification in the Marina district. *Bull Seism Soc Am* 81(5):1980–1997
- Bommer JJ, Stafford PJ, Alarcón JE, Akkar S (2007) The influence of magnitude range on empirical ground-motion prediction. *Bull Seism Soc Am* 97:2152–2170
- Caputo R (1990) Geological and structural study of the recent and active Brittle deformation of the neogene-quaternary basins of Thessaly (Greece). *Scientific Annals*, 12, Aristotle University of Thessaloniki, vol 2, 5 encl., 252 pp (Thessaloniki)
- Caputo R (1995) Inference of a seismic gap from geological data: Thessaly (Central Greece) as a case study. *Ann Geofisica* 38:1–19
- Caputo R (2005) Ground effects of large morphogenic earthquakes. *J Geodyn* 40(2–3):113–118
- Caputo R, Helly B (2000) Archéosismicité de l'Égée: Étude des failles actives de la Thessalie. *Bull Corresp Hell* 124(2):560–588 (Athens)
- Caputo R, Helly B (2005a) Archaeological evidences of past earthquakes: a contribution to the SHA of Thessaly, Central Greece. *J Earthq Eng* 9(2):199–222
- Caputo R, Helly B (2005b) The Holocene activity of the Rodia fault, Central Greece: *J Geodyn*. doi:[10.1016/j.jog.2005.07.004](https://doi.org/10.1016/j.jog.2005.07.004)
- Caputo R, Helly B (2008) The use of distinct disciplines to investigate past earthquakes. *Tectonophys*. doi:[10.1016/j.tecto.2007.05.007](https://doi.org/10.1016/j.tecto.2007.05.007)
- Caputo R, Pavlides S (1993) Late Cainozoic geodynamic evolution of Thessaly and surroundings (Central-Northern Greece). *Tectonophys* 223(3–4):339–362
- Caputo R, Bravard J-P, Helly B (1994) The Pliocene-quaternary tecto-sedimentary evolution of the Larissa Plain (Eastern Thessaly, Greece). *Geodin Acta* 7:57–85
- Caputo R, Piscitelli S, Oliveto A, Rizzo E, Lapenna V (2003) The use of electrical resistivity tomography in active tectonics. Examples from the Thyrnavos Basin, Greece. *J Geodyn* 36(1–2):19–35
- Caputo R, Helly B, Pavlides S, Papadopoulos G (2004) Palaeoseismological investigation of the Thyrnavos Fault, Central Greece. A contribution to the seismic hazard assessment of Thessaly. *Tectonophys*. doi:[10.1016/j.tecto.2004.07.047](https://doi.org/10.1016/j.tecto.2004.07.047)
- Caputo R, Helly B, Pavlides S, Papadopoulos G (2006) Archaeo- and palaeoseismological investigations in Northern Thessaly (Greece): insights for the seismic potential of the region. *Nat Haz*. doi:[10.1007/s11069-006-0023-9](https://doi.org/10.1007/s11069-006-0023-9)
- Chetouane B, Vinches M, Dubois F, Bohatier C, Devillers Ph, Nemoz-Gaillard M (2008) Analyse comparée de différentes modélisations du comportement au séisme de monuments en pierres sèches. *Actes des VI^e et VII^e Rencontres du Groupe APS*, 113–126
- Cundall PA, Strack ODL (1979) A discrete numerical model for granular assemblies. *Géotechnique* 29:47–65
- D'Asdia P, D'Ayala D (1991) L'analisi del comportamento attritivo di murature costituite da grandi blocchi a secco. *Atti del 5^o Convegno Nazionale "L'Ingegneria Sismica in Italia"*, Palermo, pp 479–490
- De Rossi MS (1874) La basilica di Santa Petronilla presso Roma, testé discoperta, caduta per terremoto. *Bull Vul Ital* 1:62–65
- Decker K, Gangl G, Kandler M (2006) The earthquake of Carnuntum in the fourth century A.D.—archaeological results, seismologic scenario and seismotectonic implications for the Vienna Basin fault, Austria. *J Seism* 10(4):479–495, Springer Netherlands
- Drakatos D, Voulgaris N, Pirlis M, Melis N, Karakostas B (2005) 3-D crustal velocity structures in Northwestern Greece. *Pure and Appl Geophys* 162:37–51
- Evans A (1928) The palace of Minos, Part 2, pp 844 (London)
- Fäh D, Steimen S, Oprsal I, Ripperger J, Wössner J, Schatzmann R, Köstli P, Spottke I, Huggenberger P (2006) The earthquake of 250 A.D. in Augusta Raurica, a real event with 3D site-effect? *J Seism* 10(4):459–477
- Galadini F, Hinzen K-G, Stiros S (eds) (2006a) Archaeoseismology: methodological issues and procedure. *J Seism* 10(4), Springer Netherlands
- Galadini F, Hinzen K-G, Stiros S (2006b) Preface. *J Seism* 10(4), Springer Netherlands
- Giuffrè A, Rovelli A, Tocchi C (1995) Effetti sismici sulle colonne coelidi di Roma: indagini numeriche e sperimentali. *Atti del 7^o Convegno Nazionale "L'Ingegneria Sismica in Italia"*, Siena, pp 1071–1080
- Grimaldi A, Luciano R, Sacco E (1991) Analisi dinamica di grandi strutture monumentali a blocchi. *Atti del 5^o Convegno Nazionale "L'Ingegneria Sismica in Italia"*, Palermo, 1421–1430
- Hinzen K-G (2005) The use of engineering seismological models to interpret archaeoseismological findings in Tolbiacum, Germany: a case study. *Bull Seism Soc Am* 95(2):521–539
- Hinzen K-G (2008) Can ruins indicate a backazimuth? *Seismol Res Lett* 79(2):290
- Hinzen K-G, Schütte S (2003) Evidence for earthquake damage on roman buildings in Cologne, Germany. *Seismol Res Lett* 74(2):124–140

- Keaton JR (1999) Synthetic seismograms for normal-faulting earthquakes using the composite source model. Report of the EERI-FEMA national earthquake hazards reduction program 1999 Professional Fellowship in Earthquake Engineering
- Kementzetzidou D (1996) Étude sismotectonique du système Thessalie-îles Sporades (Grèce centrale). Ph.D. thesis, Université J. Fourier-Grenoble I, 151 pp, Grenoble
- Knödel K, Krummel H, Lange G (1997) Geophysik—Handbuch zur Erkundung des Untergrundes von Deponien und Altlasten, Band 3, BGR. Springer, Berlin
- Korjenkov AM, Mazor E (1999) Seismogenic origin of the ancient Avdat ruins, Negev Desert, Israel. *Nat Hazards* 18:193–226
- Korjenkov AM, Arrowsmith JR, Crosby C, Mamyrov E, Orlova LA, Povolotskaya IE, Tabaldiev K (2006) Seismogenic destruction of the Kamenka medieval fortress, northern Issyk-Kul region, Tien Shan (Kyrgyzstan). *J Seism* 10(4):431–442
- Liberatore D, Larotonda A, Dolce M (1998) Dynamic analysis of voussoir arches under seismic actions. In: Proceedings of the 2nd national workshop. The protection of Cultural Heritage. The Seismic Problem, Rome, April 9–10, 1997, pp 551–571
- Mazor E, Korjenkov A (2001) Applied archaeoseismology: decoding earthquake parameters recorded in archaeological Ruins. In: Krasnov B, Mazor E (eds) *The maktsheshim country: a laboratory of nature—geological and ecological studies in the desert region of Israel*, pp 423, Pensoft (Sofia, Moscow)
- Mistler M, Butenweg C, Meskouris K (2006) Modelling methods of historic masonry buildings under seismic excitation. *J Seism* 10(4):497–510, Springer Netherlands
- Mooney WD, Laske G, Masters TG (1998) A global crustal model at $5^\circ \times 5^\circ$. *J Geophys Res* 103(B1):727–748
- Nikonov AA (1988) On the methodology of archeoseismic research into historical monuments In: Marinos PG, Koukis GC (eds) *Engineering geology of ancient works, monuments and historical sites, preservation and protection*, Balkema, Rotterdam, 1315–1320
- Nikonov AA (1996) The disappearance of the ancient towns of Dioscuria and sebastopolis in Colchis on the Black Sea: a problem in engineering geology and paleoseismology In: Stiros S, Jones RE (eds) *Archaeoseismology*, British School at Athens, fitch laboratory occasional paper 7, 195–204, The Short Run Press (Exeter)
- Oliveto A.N, Mucciarelli M, Caputo R (2004) HVSr prospections in multi-layered environments: an example from the Tyrnavos Basin (Greece). *J Seism* 8:395–406
- Pagnoni T (1995) Seismic analysis of masonry and block structures with the discrete element method. In: Proceedings of the 10th European conference on earthquake engineering, Vienna, 1669–1674
- Papaioannou I (1981) O seismos tis Larissas tou 1892 [The 1892 earthquake of Larissa]. Newspaper Eleftheria, March 15, 1981, Larissa [in Greek]
- Papazachos BC, Papazachou C (1997) The earthquakes of Greece, Editions ZITI, Thessaloniki, pp 304
- Pavlidis S, Caputo R (2004) Magnitude versus faults/surface parameters: quantitative relationships from the Aegean Region. *Tectonophys* 380:159–188
- Press F (1966) Seismic velocities—handbook of physical constants—revised edition, Section 9. The Geological Society of America Memoir, p 97
- Psycharis I, Jennings PC (1983) Rocking of slender rigid bodies allowed to uplift. *Earthq Eng and Struct Dyn* 11(1):57–76
- Reinecker J, Heidbach O, Tingay M, Sperner B, Müller B (2005) The 2005 release of the world stress map (available online at <http://www.world-stress-map.org>)
- Sarubbi P (2005) Modellazione ed analisi di strutture murarie a blocchi—Un caso studio: Il Grande Teatro di Larissa (Grecia). Tesi di Laurea, Università degli Studi della Basilicata, Facoltà di Ingegneria, 203 pp, Potenza
- Scherbaum F, Cotton F, Staedtker H (2006) The estimation of minimum-misfit stochastic models from empirical ground-motion prediction equations. *Bull Seis Soc Am* 96:427–445
- Seber D, Sandvol E, Sandvol C, Brindisi C, Barazangi M (2001) Crustal model for the middle East and North Africa region: implications for the isostatic compensation mechanism. *Geophys J Int* 147(3):630–638
- Sogreah (1974) Ground water development project of the plain of Thessaly. Final Report R. 11971, Grenoble, December 1974, unpublished
- Stiros S, Jones RE (eds) (1996) *Archaeoseismology*. British School at Athens, Fitch Laboratory occasional paper 7, 268 pp, The Short Run Press (Exeter)
- Wells DL, Coppersmith KJ (1994) New empirical relationships among magnitude, rupture length, rupture width, rupture area and surface displacement. *Bull Seism Soc Am* 84(4):974–1002
- Zelt BC, Taylor B, Sachpazi M, Hirn A (2005) Crustal velocity and Moho structure beneath the Gulf of Corinth, Greece. *Geophys J Int* 162:257–268
- Zeng Y, Anderson JG, Yu G (1994) A composite source model for computing realistic synthetic strong ground motions. *Geophys Res Lett* 21(8):725–728